OPTICS

Laser^2: A two-domain photon-phonon laser

Ning Wang[1], He Wen[1], Juan Carlos Alvarado Zacarias[1], Jose Enrique Antonio-Lopez[1], Yuanhang Zhang[1], Daniel Cruz Delgado[1], Pierre Sillard[2], Axel Schülzgen[1], Bahaa E. A. Saleh[1], Rodrigo Amezcua-Correa[1], Guifang Li[1]*

The laser is one of the greatest inventions in history. Because of its ubiquitous applications and profound societal impact, the concept of the laser has been extended to other physical domains including phonon lasers and atom lasers. Quite often, a laser in one physical domain is pumped by energy in another. However, all lasers demonstrated so far have only lased in one physical domain. We have experimentally demonstrated simultaneous photon and phonon lasing in a two-mode silica fiber ring cavity via forward intermodal stimulated Brillouin scattering (SBS) mediated by long-lived flexural acoustic waves. This two-domain laser may find potential applications in optical/acoustic tweezers, optomechanical sensing, microwave generation, and quantum information processing. Furthermore, we believe that this demonstration will usher in other multidomain lasers and related applications.

INTRODUCTION

The laser, one of the greatest inventions in history (*1*), was created as an extension of electronic oscillators at radio frequencies (RFs) and masers at microwave frequencies into the optical regime. The ensuing tremendous applications of lasers have stimulated new extensions of the concept to other physical domains, including acoustic (phonon) oscillators [also known as sasers (*2*)] and oscillators at atom/matter waves (*3*). Although the term laser traditionally means an optical oscillator based on the concept of stimulated emission, because of its ubiquity, it has been used to mean oscillator, and so, the terms phonon lasers and atom/matter lasers have been adopted. Quite often, a laser in one physical domain is pumped by energy in another physical domain. Examples include semiconductor lasers pumped by electrical current injection, and phonon lasers pumped by energy provided via stimulated Brillouin scattering (SBS) using optical lasers as pumps, and optically pumped atom lasers. However, all lasers demonstrated so far have only lased in one physical domain. While coupled electronic oscillators are routinely used and coupled photonic lasers are also constructed in the form of arrays (*4*), coupled oscillators involving different physical domains have not been demonstrated.

There are some applications where simultaneous photon and phonon lasing is useful. For example, optical trapping can only control objects on the nanometer scale (*5*), while the acoustic tweezer can control objects on the submillimeter scale (*6*). By using both optical and acoustic lasers, it is possible to provide a better range, accuracy, and resolution for the tweezers (*7*). Combined ultrasonic and photonic biological imaging would improve image quality in terms of resolution, penetration depth, and contrast (*8*, *9*). It is also possible to generate high-quality, narrow-linewidth microwave signals based on the mutual coherence between the pump, the photon laser, and the phonon laser. Because the coupled-wave equations governing the amplification of the two-domain laser (see the Supplementary Materials) are identical to those of the optical parametric amplification process, the two-domain laser can produce nonclassical states, such as squeezed/entangled states, in two domains (*10*). Correlated emission of photons and phonons may be used for applications such as heralding of a single phonon by detection of a single photon. Hence, the two-domain laser can potentially find applications in quantum information processing and sensing (*11*, *12*).

Prior work in related areas include demonstration of the phonon lasers. This is a mechanical analog of the optical laser where coherent acoustic radiation (sound wave) can be generated by using the process of sound amplification via stimulated emission of phonons. Sound waves can be described by phonons just as light waves can be considered as photons. This type of devices is capable of producing coherent acoustic oscillations with characteristics that are similar to optical lasers, such as narrow linewidth and spatial coherence. Highly coherent acoustic sources can find applications in areas including high-precision metrology (*13*–*15*), sensing (*16*, *17*), acoustic imaging (*18*, *19*), nondestructive testing (*20*), and microwave photonic signal processing (*21*–*23*). Phonon lasers have been extensively studied since 1996 after the concept was first proposed (*24*). In recent decades, several impressive experiments have been reported. The first phonon laser, producing coherent oscillation of the acoustic wave at a frequency of 441 GHz, was demonstrated using a semiconductor superlattice (*2*).

Optomechanics is a powerful tool that creates coupling between optical and mechanical waves (*11*, *25*). It provides the possibility of controlling acoustic phonons using light. For example, by using laser pumping of an Mg^+ ion, stimulated emission of center-of-mass phonons occurs, providing saturable amplification of the motion (*26*). Recently, a phonon laser was demonstrated on the basis of the oscillation of a silica nanosphere levitated in an optical tweezer under vacuum (*27*). The characteristics of an acoustic topological insulator in optomechanical crystals were found to be dependent on the amplitude and frequency of the driving laser (*28*). Fast reconfigurable nanomechanical photonic metamaterials have been envisioned recently (*29*). Optical-acoustic wave coupling can be used for parity-time (PT)–symmetric phonon lasers (*30*) and investigating the PT-symmetry–breaking phase chaos in optomechanical systems (*31*). SBS is known as a strong nonlinear effect

[1]CREOL, The College of Optics and Photonics, University of Central Florida, Orlando, FL, 32816, USA. [2]Prysmian Group, Parc des Industried Artois Flandres, Douvrin 62138, France.
*Corresponding author. Email: li@ucf.edu

that can be described as an interaction between light and sound waves (*32*). Acoustic phonons can be amplified through the SBS process using optical pumping. Phonon lasing action at a frequency of 23 MHz was observed in a compound microcavity, based on the SBS between two supermodes in coupled microtoroids that operates in close analogy to a two-level laser system (*33*). Excitation of whispering-gallery mechanical resonances ranging from 49 to 1400 MHz by using forward SBS between different transverse optical modes in a silica microsphere resonator was reported (*34*). A phonon laser of Hermite-Gaussian–like acoustic modes was also demonstrated on the basis of backward SBS in a TeO_2 crystal at cryogenic temperatures (*35*). Another phonon laser with an oscillation frequency of 100 MHz was demonstrated in a multicore fiber, in an optoelectronic oscillator structure with intercore optical-mechanical cross-talk as the feedback mechanism (*36*).

In all previous demonstrations, the Stokes optical (acoustic) wave was merely a byproduct in a phonon (photon) laser. Here, we report a system of coupled oscillators lasing in two distinct physical domains, pumped by the same source. We have experimentally demonstrated simultaneous photon and phonon lasing in a two-mode silica fiber ring cavity based on the forward intermodal SBS mediated by long-lived flexural acoustic waves. Our experimental results show that two-domain concurrent photon and phonon lasing enhance the output powers of both phonon and photon lasers.

Operation principle

The two-domain laser reported here produces simultaneous phonon and photon lasing in a common (fiber ring) cavity. The low-frequency flexural acoustic wave is generated via forward SBS between the fundamental LP_{01} and a higher-order LP_{11} transverse optical modes in a two-mode fiber (TMF) (*37*, *38*). Actually, both backward and forward SBS happen in a few-mode fiber (FMF), but they are mediated by two different types of acoustic waves. For both backward and forward SBS processes, energy and momentum must be conserved. The dispersion diagram with energy and momentum conservation for backward SBS is shown in Fig. 1B. The blue and red lines are the dispersion curves of the forward and backward optical waves, respectively, and the green line is the dispersion curve of the acoustic mode. The scattered Stokes wave propagates in the backward direction, while the acoustic wave is in the forward direction. The emitted acoustic modes are longitudinal modes confined inside the fiber core area. Their frequencies are on the order of 10 GHz. In silica, the acoustic waves at such high frequencies are highly damped with a phonon lifetime of only ~10 ns, corresponds to a propagation length of 60 μm. These highly damped acoustic phonons are absorbed by the material immediately, unable to create effective acoustic feedback. In strong contrast, for the forward SBS shown in Fig. 1C, both the Stokes wave and the acoustic wave propagate in the forward direction. The acoustic flexural modes are generated via the intermodal SBS between two different transverse optical modes. In this case, the emitted phonon frequencies can drop to the megahertz range. These low-frequency phonons, confined in the entire structure (core and cladding) of the silica fiber, have a much longer lifetime (*33*), typically on the order of 10 ms. Their propagation length is more than 10 m, which makes it possible for the phonons to lase as well. The Supplementary Materials provides more details on the optical and acoustic properties of the fiber.

A schematic of the phonon and photon laser in a TMF ring cavity is shown in Fig. 1A. By using the fundamental LP_{01} mode as the pump, both the LP_{11} Stokes optical wave and the flexural acoustic wave are amplified and resonantly oscillate inside the same ring cavity. The coherent oscillation of the optical wave enhances the gain of acoustic phonons and vice versa, leading to simultaneous lasing in two domains. We experimentally demonstrate such a two-domain fiber laser using a 10-m reduced-cladding TMF. Four states of operation were observed in this device as the optical pump power was increased. To produce simultaneous photon and phonon lasing, the gains for both the Stokes optical wave and the acoustic wave must exceed their losses. In our demonstration, the forward intermodal SBS occurs inside the 10-m TMF, and both the LP_{11} Stokes optical wave and flexural acoustic wave are amplified because of the low loss of the acoustic wave. This is hardly achieved in the backward SBS process. The LP_{11} Stokes optical wave is partially coupled out of the cavity through a fiber coupler. The

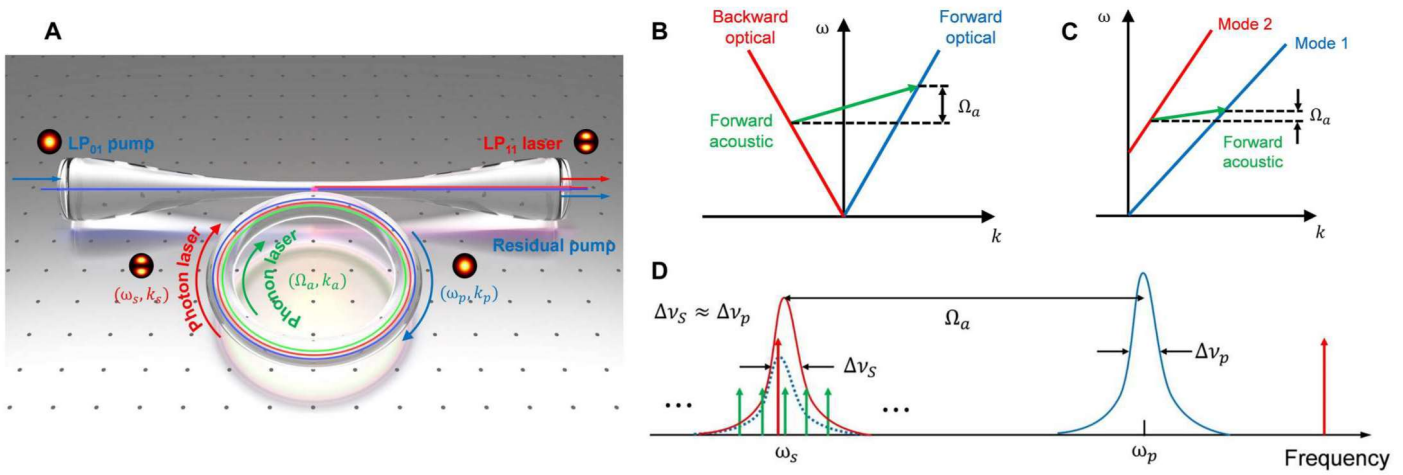

Fig. 1. Operation principle of the two-domain fiber laser. (**A**) Schematic of the two-domain (phonon and photon) laser based on forward intermodal SBS in a TMF ring cavity. Dispersion diagrams with energy and momentum conservation conditions for (**B**) backward SBS and (**C**) forward SBS in optical fiber. (**D**) Working principle of simultaneous phonon and phonon lasing illustrated in the frequency domain.

optical power split ratio of the fiber coupler can be independently controlled by adjusting the length of the taper waist of the fiber coupler. In this experiment, the length of the taper waist is adjusted such that the LP_{01} optical pump operates predominantly in the cross state and the LP_{11} Stokes optical wave in the bar state, thereby facilitating pump power injection and Stokes optical wave lasing. In addition, we used two fibers with the same core size but different cladding sizes. This choice breaks the degeneracy of the acoustic modes in the two fibers so that the TMF coupler operates in the bar state for the acoustic wave inside the cavity. When the difference between the acoustic wave vectors of the two fibers is large enough, the structure functions like an asymmetric Y junction in the acoustic domain, and the acoustic field is confined in the same fiber throughout the coupler (*39*). This allows the phonon energy to stay inside the ring cavity to facilitate phonon lasing. In the future, another coupler that maintains symmetry in the acoustic domain but breaks symmetry in the optical domain can be used as a phonon laser output coupler. In addition, Once the phase-matching conditions are satisfied for both photon and phonon waves, the intracavity powers for both will increase until the saturated gain equals the roundtrip loss. In the steady state, the flexural acoustic wave and the Stokes optical wave resonantly oscillate inside the fiber ring cavity. The phonon laser power is confined inside the cavity, while the Stokes optical laser is observed at the output of the coupler.

The operation principle of the two-domain laser is elucidated in the frequency domain, as depicted in Fig. 1D. The LP_{01} pump laser (blue curve) has a central wavelength of 976 nm with a 3-dB linewidth $\Delta\upsilon_p$ of ~1 MHz. It creates a forward SBS gain peak with a frequency downshift for the LP_{11} Stokes wave (blue dashed curve). We selected the lowest-order flexural acoustic mode for the phonon laser because it has no cutoff and, therefore, can propagate through the fiber coupler region. The free spectral range (FSR) of the ring TMF cavity for the LP_{11} optical mode is around 20 MHz (red arrows), which is larger than the Brillouin gain bandwidth. To satisfy the roundtrip resonance condition for the optical laser, the pump frequency is gradually swept to align the gain peak with one of the longitudinal modes for the LP_{11} Stokes optical wave. The FSR of the acoustic mode is less than 200 Hz (green arrows), and therefore, many acoustic modes can be found within the SBS gain bandwidth. Hence, it is relatively easy to satisfy the roundtrip resonance condition for the phonon laser. When both photons and phonons are lasing, a strong peak for the optical laser will appear (red curve). The frequency difference between the photon laser and the pump is the phonon laser frequency Ω_a. Unlike the backward SBS-based fiber lasers, where the laser linewidth is compressed compared to the pump, this forward SBS-based photon laser has a similar linewidth as its pump due to the ultralow dissipation rate of the acoustic phonons. However, the phonon laser does have an ultranarrow emission linewidth, which means that the Stokes optical laser is extremely coherent with the pump.

RESULTS

The experimental setup of the photon and phonon two-domain laser is shown in Fig. 2A. A 976-nm fiber-coupled pump diode has a linewidth of ~1 MHz with a maximum output power of 400 mW. A thermoelectric cooler controller was used to precisely control the operating temperature with a step size of 0.001°C. The pump in the fundamental mode was launched into the TMF with an 80-μm outer diameter and completely coupled into the 60-μm outer diameter TMF ring cavity through the TMF coupler. A polarization controller was used to optimize the pump power that is coupled into the fiber ring cavity. The forward intermodal SBS took place in the 10-m TMF of which the coating was stripped off to prevent the absorption of the acoustic wave. Both the LP_{11} Stokes optical wave and the flexural acoustic wave traveling clockwise were amplified. The pump frequency was tuned by controlling the pump laser operating temperature. The LP_{11} Stokes photon laser was partially coupled out through the TMF coupler together with the residual LP_{01} pump. It should be noted that although the photon laser belongs to a different spatial mode, it is still highly coherent with the pump in temporal domain. We used a low–cross-talk three-mode mode-selective photonic lantern (MSPL) to separate the pump and the Stokes wave and convert the photon laser back into the fundamental mode at the same time. We measured the optical power of the LP_{11} Stokes photon laser. In addition, we characterized the beat-note electrical spectrum between the pump and the Stokes photon laser by using an electrical spectrum analyzer. A variable optical attenuator was used to attenuate input power below the saturation power of the photodetector.

The fiber used to provide the gain in this experiment was a reduced-cladding TMF, made of pure silica cladding with GeO_2-doped silica core. The measured fiber refractive index profile is shown in Fig. 2B, and its cross-sectional microscopic image is shown in Fig. 2C. The core and cladding diameters are 6.8 and 60 μm, respectively. It has a step-index–shaped profile with a numerical aperture of 0.13, corresponding to a fiber V number of 2.83, ensuring that it supports two LP modes at the operation wavelength. The measured intensity profiles of three guided modes supported by this TMF at λ = 976 nm are shown in Fig. 2D. The first-order flexural acoustic mode that mediates the forward SBS between the two optical modes has a frequency of 5.11 MHz. The intrinsic damping rate of the acoustic wave at this frequency in silica is only 36 Hz, which is smaller than the acoustic FSR of the cavity and is low enough to form discrete acoustic cavity modes. Because the acoustic field extends into the entire cladding, reducing the TMF cladding size can improve the overlap between the acoustic and optical fields and thereby increase the SBS gain coefficient.

Figure 3A shows the measured LP_{11} photon laser output power as a function of pump power injected into the ring cavity. The inset shows the output power, in logarithmic scale, as a function of the pump power injected into the ring cavity. Two thresholds are clearly seen, corresponding to the photon laser and the phonon laser. The Stokes photon laser starts lasing before the phonon laser because the small-signal gain for the Stoke wave is higher. The threshold pump power of the photon laser was 180 mW. However, because of the weak acoustic power, the output photon laser power was low, only a few milliwatts. When the pump power was increased to around 308 mW, the phonon laser started lasing as well. A stronger acoustic field also enhanced the gain of the Stokes wave. The slope of the photon laser output power became much steeper in this region. The maximum measured photon laser power was 21.8 mW at a pump power of 367 mW. The measured threshold pump power and output laser power agree with the numerical simulation results (see the Supplementary Materials).

We also studied the power of the RF beat note between the pump and Stokes photon laser as a function of pump power, as shown in a

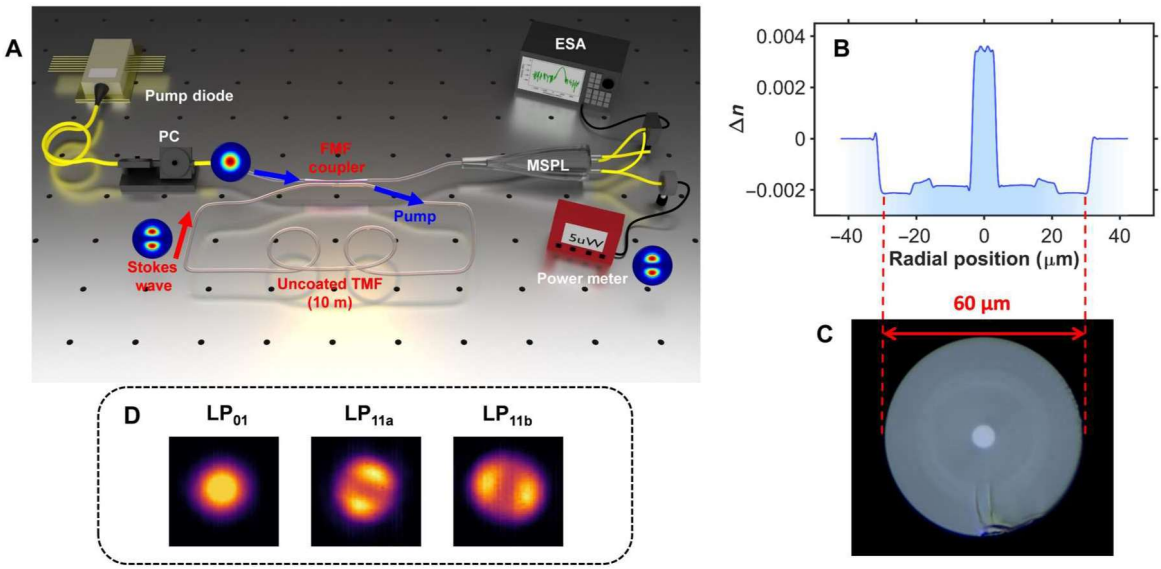

Fig. 2. Experimental setup. (**A**) Experimental setup for demonstrating two-domain, simultaneous phonon and photon lasing based on forward intermodal SBS in a 10-m TMF ring cavity. (**B**) Measured refractive index profile of the reduced-cladding TMF used as the gain media in the two-domain (phonon and photon) laser. (**C**) Microscope cross-sectional image of the TMF. (**D**) measured mode profiles of the three guided optical modes of the TMF at λ = 976 nm.

log-linear scale in Fig. 3B. The power of this RF beat note theoretically increases by the same order of magnitude as the intracavity phonon laser power (see the Supplementary Materials), and they have exactly the same threshold pump power. Because a direct measurement of the vibration amplitude of the sound wave would necessitate microscopic imaging at megahertz frame rates, which is not readily available, the RF beat-note measurement is an effective substitute for a direct measurement. It is shown in the figure that there are two jumps in the RF peak power that correspond to the thresholds of photon and phonon lasers. When Fig. 3B is replotted using a linear scale for the RF power (vertical axis) versus the squared pump power (horizontal axis), shown in Fig. 3C, four slopes corresponding to those in Fig. 3A are also observed.

We recorded the beat-note electrical spectra at several pump power levels, corresponding to the circles in Fig. 3 (A and B). The evolution of electrical spectral lineshape with the pump powers can be observed. Figure 3D shows that at a pump power near 100 mW the cavity operates in the spontaneous Brillouin scattering regime, and the beat-note spectrum has a 3-dB linewidth of approximately 2.2 MHz at a central frequency of 5.4 MHz. Figure 3E shows that at a pump power near 161 mW, the cavity starts to operate predominantly in the forward SBS regime, and the beat-note spectrum has a reduced 3-dB linewidth of 1.6 MHz. Figure 3F shows that at a pump power of 271 mW, the cavity operates in the Stokes photon lasing regime, and the beat-note spectrum reveals a strong peak at the center frequency of 5.6 MHz with a 3-dB linewidth of approximately 26 kHz. Figure 3G shows that at the pump power of 367 mW, the cavity operates in the simultaneous phonon and photon lasing regime, and the beat-note spectrum reveals an even stronger peak at the center frequency of 5.2 MHz, with a 3-dB linewidth of only 1.7 kHz, corresponding to the linewidth of the phonon laser. Thus, two-domain lasing resulted in an order-of-magnitude narrowing of the phonon emission linewidth compared to that in the photon-only lasing, which is hardly achieved by using existing acoustic techniques.

The phonon-photon laser in this work represents an inverted dissipative hierarchy in which the acoustic emission linewidth is much narrower than the pump laser linewidth, as opposed to the standard dissipative hierarchy of the backward SBS lasers (*40*). At low pump powers, spontaneous Brillouin scattering is mediated by many longitudinal acoustic modes. In the SBS and photon lasing regimes, as the finesse of the acoustic cavity increases, the bandwidth correspondingly decreases, resulting in the narrowing of the spectrum of the phonons, and thus the pump-Stokes beat-note linewidth. The pump-Stokes beat-note linewidth in the simultaneous photon-phonon lasing regime is further reduced because even a smaller number of longitudinal acoustic modes can lase. The beat-note linewidth in the simultaneous photon-phonon lasing regime is still wider than the acoustic damping rate, indicating that phonon laser is still multimode.

DISCUSSION

While coherently coupled lasers, such as laser diode arrays, are an established technology, coupled lasing in different physical domains in the same cavity is a physical phenomenon that has not yet been observed. The two-domain laser reported in this article exploits forward intermodal SBS to enable the coupling necessary for concurrent photon and phonon lasing in the same cavity. In our experiment, this was a 10-m reduced-cladding TMF in a ring laser configuration. The measured LP_{11} Stokes photon laser power was more than 20 mW, and the phonon laser linewidth was on the order of 1 kHz. Photon lasing was observed by direct measurement of the dependence of photon laser power on the pump power. The phonon laser power was not observed directly because high-resolution and high frame rate (~5 MHz) cameras are not yet available. Instead, the phonon laser power was estimated by measurement of the RF power of the beat signal between the pump and the laser light. Nevertheless, observation of the four regimes of laser operation corresponding to the spontaneous Brillouin scattering, the

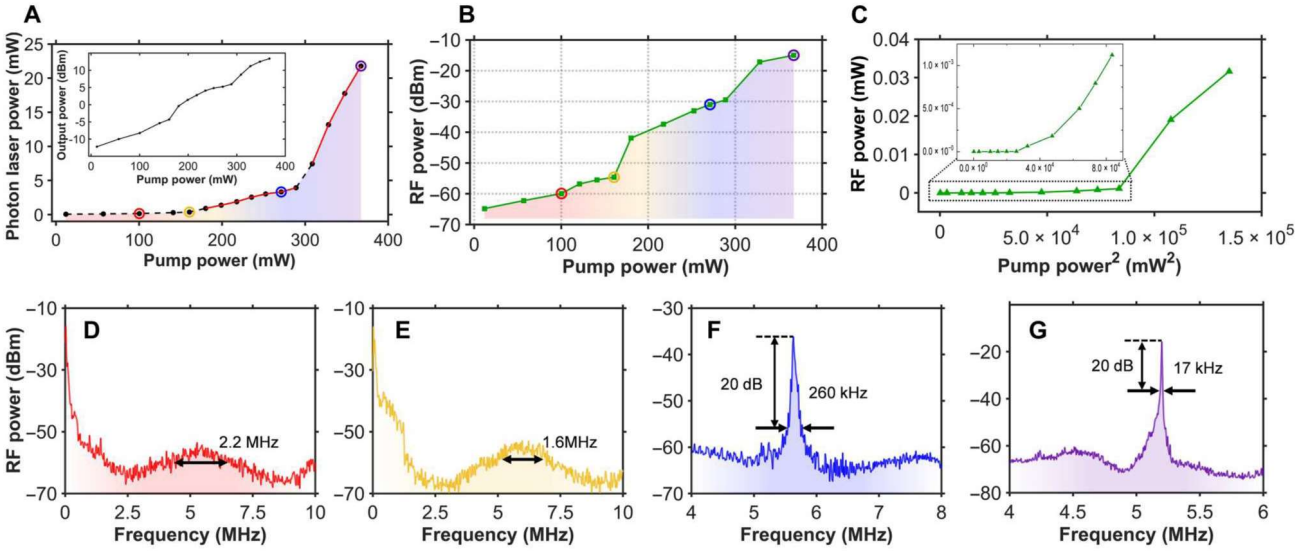

Fig. 3. Experimental results. (**A**) Measured optical power of the LP_{11} Stokes photon laser versus injected pump power, (inset) optical power in log scale. (**B**) RF power of the beat note between the pump and the Stokes photon laser at each pump power. (**C**) RF power in linear scale versus squared pump power and beat-note electrical spectra at a pump power of (**D**) 100 mW, (**E**) 161 mW, (**F**) 271 mW, and (**G**) 367 mW, color-matched to the circles in (A) and (B).

SBS, photon lasing, and photon-phonon lasing aligns with our theoretical model of two-domain lasing.

A source of two coherently coupled lasers in different physical domains has potential for numerous applications. Because light and sound have distinct spatial and temporal properties and interact with materials differently, their concurrent availability can be exploited in various ways. Potential applications include acoustic and optical trapping at different physical scales, concurrent photoacoustic imaging of optomechanical and optical properties of objects, and controlled generation of high-quality microwave signals. It could also lead to future advances in optomechanics. Envisioned applications in quantum information processing include generation of photon-phonon entangled and squeezed states, as well as more versatile coherent control and characterization of quantum states in both domains. We believe that our work will usher in other multidomain lasers and related applications.

MATERIALS AND METHODS

Bare fiber handling

The original two-mode FMF has a 150-μm-diameter acrylate coating. To completely remove the coating of the 10-m FMF, we soaked the entire 10-m fiber in acetone for ~72 hours. Any residual coating can be easily removed using a blade. It is noted that the container of the acetone should be isolated from the air, otherwise the acetone will be vapored quickly. Cleaving of the fiber can be done by using regular fiber cleavers (e.g., Fujikura CT-30). It is necessary to set the fiber outer diameter to be 60 to 80 μm using the adjuster.

For the splicing of the reduced cladding FMF, we used a commercial portable fusion splicer (INNO View3). To splice two fibers with a 60-μm outer diameter, the arc power and arc time must be reduced. The cleaning arc time should be no more than 80 ms. The pre-arc power was set to be 50% of the standard value and the pre-arc time to be 120 ms. The fuse arc power was set to be 70% of the standard value, and its time was 1500 ms. The splice loss was measured to be only 0.1 dB.

MSPL demultiplexer

We used a MSPL to separate the laser and the residual pump, which have different LP modes. MSPLs are passive all-fiber devices capable of efficiently multiplexing single-mode inputs and converting each input into a specific LP mode at the output. They are widely used as mode (de)multiplexer in mode-division multiplexing fiber communication systems (*41*). In general, a photonic lantern consists of multiple-input single-mode fibers (SMFs) inserted into a fluorine-doped capillary tube whose refractive index is lower than that of the SMF cladding. The tube is adiabatically tapered down to create an FMF output at the taper waist. The optical modes are confined in the cladding area guided by the low index capillary. Mode selectivity can be obtained if the input SMF core radii are deliberately chosen. Each input fundamental mode evolves into a particular mode in the output FMF with a matched propagation constant (*42*, *43*).

For the three-mode MSPL used in this experiment, it contains three graded-index input fibers with different core diameters. The one with an 18-μm core diameter is matched to the LP_{01} mode; the other two with a 14-μm core diameter are matched to the LP_{11} modes. After tapering, the resultant FMF has core and cladding diameters of 18 and 90 μm, respectively. We measured the mode intensity profile of each LP mode at the output of the MSPL at a wavelength λ = 976 nm, the three lowest order LP modes were generated successfully. We also measured the insertion losses of this MSPL without splice with the 80-μm cladding diameter TMF. The insertion losses of LP_{01}, LP_{11a}, and LP_{11b} modes are 1.17, 1.51, and 1.49 dB, respectively.

Supplementary Materials

This PDF file includes:

Supplementary Text
Figs. S1 to S8
References

REFERENCES AND NOTES

1. J. P. Gordon, H. J. Zeiger, C. H. Townes, The maser—New type of microwave amplifier, frequency standard, and spectrometer. *Phys. Rev.* **99**, 1264–1274 (1955).
2. R. Beardsley, A. Akimov, M. Henini, A. Kent, Coherent terahertz sound amplification and spectral line narrowing in a stark ladder superlattice. *Phys. Rev. Lett.* **104**, 085501 (2010).
3. G. Cennini, G. Ritt, C. Geckeler, M. Weitz, All-optical realization of an atom laser. *Phys. Rev. Lett.* **91**, 240408 (2004).
4. Z. Gao, S. Fryslie, B. J. Thompson, P. S. Carney, K. D. Choquette, Parity-time symmetry in coherently coupled vertical cavity laser arrays. *Optica* **4**, 323–329 (2017).
5. A. Ashkin, J. M. Dziedzic, J. E. Bjorkholm, S. Chu, Observation of a single-beam gradient force optical trap for dielectric particles. *Opt. Lett.* **11**, 288 (1986).
6. B. W. Drinkwater, Dynamic-field devices for the ultrasonic manipulation of microparticles. *Lab Chip* **16**, 2360–2375 (2016).
7. G. Thalhammer, R. Steiger, M. Meinschad, M. Hill, S. Bernet, M. Ritsch-Marte, Combined acoustic and optical trapping. *Biomed. Opt. Express* **2**, 2859–2870 (2011).
8. T. Harrison, J. C. Ranasinghesagara, H. Lu, K. Mathewson, A. Walsh, R. J. Zemp, Combined photoacoustic and ultrasound biomicroscopy. *Opt. Express* **17**, 22041 (2009).
9. J. James, V. M. Murukeshan, L. S. Woh, Integrated photoacoustic, ultrasound and fluorescence platform for diagnostic medical imaging-proof of concept study with a tissue mimicking phantom. *Biomed. Opt. Express* **5**, 2135–2144 (2014).
10. R. Riedinger, S. Hong, R. A. Norte, J. A. Slater, J. Shang, A. G. Krause, V. Anant, M. Aspelmeyer, S. Gröblacher, Non-classical correlations between single photons and phonons from a mechanical oscillator. *Nature* **530**, 313–316 (2016).
11. F. Marquardt, S. M. Girvin, Trend: Optomechanics. *Phys. Ther.* **2**, 40 (2009).
12. K. Stannigel, P. Komar, S. J. M. Habraken, S. D. Bennett, M. D. Lukin, P. Zoller, P. Rabl, Optomechanical quantum information processing with photons and phonons. *Phys. Rev. Lett.* **109**, 013603 (2012).
13. G. Ranjit, M. Cunningham, K. Casey, A. A. Geraci, Zeptonewton force sensing with nanospheres in an optical lattice. *Phys. Rev. A* **93**, 053801 (2016).
14. D. Hempston, J. Vovrosh, M. Toroš, G. Winstone, M. Rashid, H. Ulbricht, Force sensing with an optically levitated charged nanoparticle. *App. Phys. Lett.* **111**, 133111 (2017).
15. A. A. Geraci, S. B. Papp, J. Kitching, Short-range force detection using optically cooled levitated microspheres. *Phys. Rev. Lett.* **105**, 101101 (2010).
16. Y. Antman, A. Clain, Y. London, A. Zadok, Optomechanical sensing of liquids outside standard fibers using forward stimulated Brillouin scattering. *Optica* **3**, 510–516 (2016).
17. D. M. Chow, Z. Yang, M. A. Soto, L. Thévenaz, Distributed forward Brillouin sensor based on local light phase recovery. *Nat. Commun.* **9**, 2990 (2018).
18. P. N. Wells, Ultrasonic imaging of the human body. *Rep. Prog. Phys.* **62**, 671–722 (1999).
19. J. Ophir, S. K. Alam, B. Garra, F. Kallel, E. Konofagou, T. Krouskop, T. Varghese, Elastography: Ultrasonic estimation and imaging of the elastic properties of tissues. *Proc. Inst. Mech. Eng. H* **213**, 203–233 (1999).
20. J. Blitz, G. Simpson, *Ultrasonic methods of non-destructive testing* (Springer Science & Business Media, 1995), vol. 2.
21. X. S. Yao, Brillouin selective sideband amplification of microwave photonic signals. *IEEE Photon. Technol. Lett.* **10**, 138–140 (1998).
22. A. Loayssa, F. J. Lahoz, Broad-band RF photonic phase shifter based on stimulated Brillouin scattering and single-sideband modulation. *IEEE Photon. Technol. Lett.* **18**, 208–210 (2006).
23. Y. Stern, K. Zhong, T. Schneider, R. Zhang, Y. Ben-Ezra, M. Tur, A. Zadok, Tunable sharp and highly selective microwave-photonic band-pass filters based on stimulated Brillouin scattering. *Photonics Res.* **2**, B18 (2014).
24. S. Wallentowitz, W. Vogel, I. Siemers, P. E. Toschek, Vibrational amplification by stimulated emission of radiation. *Phys. Rev. A* **54**, 943–946 (1996).
25. T. J. Kippenberg, K. J. Vahala, Cavity optomechanics: Back-action at the mesoscale. *Science* **321**, 1172–1176 (2008).
26. K. Vahala, M. Herrmann, S. Knünz, V. Batteiger, G. Saathoff, T. W. Hänsch, T. Udem, A phonon laser. *Nat. Phys.* **5**, 682–686 (2009).
27. R. M. Pettit, W. Ge, P. Kumar, D. R. Luntz-Martin, J. T. Schultz, L. P. Neukirch, M. Bhattacharya, A. N. Vamivakas, An optical tweezer phonon laser. *Nat. Photon.* **13**, 402–405 (2019).
28. V. Peano, C. Brendel, M. Schmidt, F. Marquardt, Topological phases of sound and light. *Phys. Rev. X* **5**, 031011 (2015).
29. N. I. Zheludev, E. Plum, Reconfigurable nanomechanical photonic metamaterials. *Nat. Nanotechnol.* **11**, 16–22 (2016).
30. H. Jing, S. K. Özdemir, X. Y. Lü, J. Zhang, L. Yang, F. Nori, PT-symmetric phonon laser. *Phys. Rev. Lett.* **113**, 053604 (2014).
31. X.-Y. Lü, H. Jing, J.-Y. Ma, Y. Wu, PT-symmetry-breaking chaos in optomechanics. *Phys. Rev. Lett.* **114**, 253601 (2015).
32. A. Kobyakov, M. Sauer, D. Chowdhury, Stimulated Brillouin scattering in optical fibers. *Adv. Opt. Photon.* **2**, 1–59 (2010).
33. I. S. Grudinin, H. Lee, O. Painter, K. J. Vahala, Phonon laser action in a tunable two-level system. *Phys. Rev. Lett.* **104**, 083901 (2010).
34. G. Bahl, J. Zehnpfennig, M. Tomes, T. Carmon, Stimulated optomechanical excitation of surface acoustic waves in a microdevice. *Nat. Commun.* **2**, 403 (2011).
35. W. H. Renninger, P. Kharel, R. O. Behunin, P. T. Rakich, Bulk crystalline optomechanics. *Nat. Phys.* **14**, 601–607 (2018).
36. H. H. Diamandi, Y. London, G. Bashan, A. Bergman, A. Zadok, Highly-coherent stimulated phonon oscillations in a multi-core optical fiber. *Sci. Rep.* **8**, 9514 (2018).
37. P. S. J. Russell, D. Culverhouse, F. Farahi, Experimental observation of forward stimulated Brillouin scattering in dual-mode single-core fibre. *Electron. Lett.* **26**, 1195–1196 (1990).
38. P. S. J. Russell, D. Culverhouse, F. Farahi, Theory of forward stimulated Brillouin scattering in dual-mode single-core fibers. *IEEE J. Quantum Electron.* **27**, 836–842 (1991).
39. N. Riesen, J. D. Love, Design of mode-sorting asymmetric Y-junctions. *Appl. Optics* **51**, 2778–2783 (2012).
40. N. T. Otterstrom, R. O. Behunin, E. A. Kittlaus, Z. Wang, P. T. Rakich, A silicon Brillouin laser. *Science* **360**, 1113–1116 (2018).
41. S. G. Leon-Saval, N. K. Fontaine, R. Amezcua-Correa, Photonic lantern as mode multiplexer for multimode optical communications. *Opt. Fiber Technol.* **35**, 46–55 (2017).
42. S. G. Leon-Saval, N. K. Fontaine, J. R. Salazar-Gil, B. Ercan, R. Ryf, J. Bland-Hawthorn, Mode-selective photonic lanterns for space-division multiplexing. *Opt. Express* **22**, 1036–1044 (2014).
43. S. Yerolatsitis, I. Gris-Sánchez, T. Birks, Adiabatically-tapered fiber mode multiplexers. *Opt. Express* **22**, 608–617 (2014).
44. R. N. Thurston, Elastic waves in rods and clad rods. *J. Acoust. Soc. Am.* **64**, 1–37 (1978).
45. C. Krischer, Optical measurements of ultrasonic attenuation and reflection losses in fused silica. *J. Acoust. Soc. Am.* **48**, 1086–1092 (1970).
46. R. G. Smith, Optical power handling capacity of low loss optical fibers as determined by stimulated Raman and Brillouin scattering. *Appl. Optics* **11**, 2489–2494 (1972).
47. T. Birks, P. S. J. Russell, C. Pannell, Low power acousto-optic device based on a tapered single-mode fiber. *IEEE Photon. Technol. Lett.* **6**, 725–727 (1994).
48. R. W. Boyd, K. Rzaewski, P. Narum, Noise initiation of stimulated Brillouin scattering. *Phys. Rev. A* **42**, 5514–5521 (1990).
49. G. P. Agrawal, Nonlinear fiber optics, (Academic Press, ed. 5, 2012), Chap. 9.
50. 24.W. Schmid, C. Jung, B. Weigi, G. Reiner, R. Michalzik, K. J. Ebeling, Delayed self-heterodyne linewidth measurement of VCSELs. *IEEE Photon. Technol. Lett.* **8**, 1288–1290 (1996).

Acknowledgments

Funding: This work was supported in part by the Army Research Office nos. W911NF-17-10553 and W911NF-20-10085 and the National Science Foundation nos. ECCS-1808976 and ECCS-1932858. **Author contributions:** Conceptualization: G.L. Methodology: N.W., H.W., Y.Z., A.S., R.A.-C., and G.L. Experiment: N.W., J.C.A.Z., J.E.A.-L., and P.S. Funding acquisition: G.L. and R.A.-C. Project administration: G.L. Supervision: G.L. and R.A.-C. Writing—original draft: N.W., G.L., and B.E.A.S. Writing—review and editing: N.W., H.W., D.C.D., G.L., B.E.A.S., and R.A.-C. **Competing interests:** The authors declare that they have no competing interests. **Data and materials availability:** All data needed to evaluate the conclusions in the paper are present in the paper and/or the Supplementary Materials.

Submitted 20 January 2023
Accepted 30 May 2023
Published 30 June 2023
10.1126/sciadv.adg7841